01 Jan 2021

Unsteady-State Contact Angle Hysteresis during Droplet Oscillation in Capillary Pores: Theoretical Model and VOF Simulation -- Supporting Information

Chao Zeng

Wen Deng
Missouri University of Science and Technology, wendeng@mst.edu

Lichun Wang

Unsteady-State Contact Angle Hysteresis during Droplet Oscillation in Capillary Pores: Theoretical Model and VOF Simulation -- Supporting Information

Abstract

Contact angle hysteresis (CAH) is a critical phenomenon that could significantly affect the fate of immiscible bubbles/droplets in vadose zones, nonaqueous phase liquid contaminated aquifers, and saline aquifers for CO_2 sequestration in terms of infiltration patterns and residual trapping mechanisms. When external physical impacts such as oscillatory excitation or pulse forcing are applied, it could result in pinned oscillation of droplets due to this CAH. Conventional steady-state analysis of contact angle could underestimate CAH. As the first time to take unsteady-state effect into consideration, a hydrodynamic analysis is developed in this study to address the unsteady-state CAH theoretically, and validated against volume-of-fluid based computational fluid dynamics simulations. It is found that the unsteady-state CAH of drop can significantly lower the critical acceleration amplitude of excitation to achieve the depinning of contact lines of drops.

Viewing Instructions

Download and view the Data spreadsheet of Figures 2-11.

Keywords and Phrases

Contact Angle Hysteresis; Pinning; Unsteady-State Response; Drop Oscillation; VOF Simulation

Disciplines

Geophysics and Seismology | Geotechnical Engineering

Comments

A spreadsheet titled 'data.xlsx' is contained in this Supporting Information in a separate file. The spreadsheet includes the data of Figures 2-11 in manuscript. In that file, all data are presented in the same tab and ordered in the same sequence as manuscript. The figure legend and x-y titles are also listed. If there is any question about the data file, feel free to contact the corresponding author Dr. Wen Deng.

Supporting information was updated Feb 2021.

[Water Resources Research]

Supporting Information for

Unsteady-state contact angle hysteresis during droplet oscillation in capillary pores: Theoretical model and VOF simulation

Chao Zeng[1], Wen Deng[1*], Lichun Wang[2]

[1]Department of Civil, Architectural and Environmental Engineering, Missouri University of Science and Technology, Rolla, MO, USA

[2]Institute of Surface-Earth System Science, Tianjin University, Tianjin, China

*Corresponding author: Wen Deng (wendeng@mst.edu)

Linear Approximation

To obtain the analytical solution of this oscillatory problem by an approximation, the capillary force difference needs to firstly be linearized. For the right interface, the capillary pressure is:

$$P_c^+ = \frac{2\sigma cos\theta^+}{R} \quad \text{(SI1)}$$

The volume of right spherical cap is:

$$V(\theta^+) = \frac{\pi R^3(2+sin\theta^+)cos\theta^+}{3(1+sin\theta^+)^2} \quad \text{(SI2)}$$

When the mean displacement $x(t)$ is small, the linearization can be applied on the Eq. (SI1) to yield:

$$\frac{dP_c^+}{dx} = \frac{dP_c^+}{d\theta^+}\left(\frac{dV(\theta^+)}{d\theta^+}\right)^{-1}\frac{dV}{dx} = \frac{2\sigma sin\theta_0(1+sin\theta_0)^2}{R^2} \quad \text{(SI3)}$$

The θ_0 in Eq. (SI3) is the equilibrium contact angle before motion, which is a constant. Therefore, the capillary pressure across the right meniscus is linearized. It is noted that the linear relationship $P_c^+ = \frac{dP_c^+}{dx}x$ holds under the linearization from Eq. (SI3). In comparison to Eq. (SI1), the linear relation of x and θ^+ can be readily attained. However, the complete relation of x and θ^+ is given by Eq. (17). Therefore, the condition of linearization can refer to Eq. (17). By plotting Eq. (17), it shows that θ^+ - θ_0 < 20° is the condition for the validity of linearization of Eq. (SI3) with error less than 5%. Consequently, the oscillation at which the contact angle variation (θ^+ - θ_0) is less than 20° can be called small oscillation,

since the linearization is applicable at this condition. If the oscillation causes larger contact angle variation, it is called large oscillation.

Similarly, the capillary pressure across the left meniscus can also be linearized. The difference of two capillary pressure is:

$$P_c^- - P_c^+ = -\frac{4\sigma sin\theta_0(1+sin\theta_0)^2}{R^2}x \quad \text{(SI4)}$$

Substituting Eq. (SI4) into Eq. (20), the new governing equation becomes:

$$\rho_o L_o \frac{d^2x}{dt^2} + \left\{2\rho_o\omega L_o\mathcal{H}_1(x) + \rho_w\omega L_w Re\left\{\frac{i\cdot J_0\left(\sqrt{i^3\omega/\omega_c^W}\right)}{J_2\left(\sqrt{i^3\omega/\omega_c^W}\right)}\right\}\right\}\frac{dx}{dt} + \frac{4\sigma}{R^2}sin\theta_0(1+sin\theta_0)^2x = (\rho_o L_o + \rho_w L_w)Asin(\omega t) \quad \text{(SI5)}$$

This equation is linear equation of dependent variable x now. It can be analyzed by an analogy to linear oscillator. For a succinct expression of notations, the new variables are defined as:

$$c = \frac{1}{\rho_o L_o}\left\{2\rho_o\omega L_o\mathcal{H}_1(x) + \rho_w\omega L_w \mathrm{Re}\left\{\frac{i\cdot J_0\left(\sqrt{i^3\omega/\omega_c^W}\right)}{J_2\left(\sqrt{i^3\omega/\omega_c^W}\right)}\right\}\right\} \quad \text{(SI6)}$$

$$\omega_0^2 = \frac{4\sigma}{\rho_o L_o R^2}sin\theta_0(1+sin\theta_0)^2 \quad \text{(SI7)}$$

$$A_0 = \frac{(\rho_o L_o + \rho_w L_w)}{\rho_o L_o}A \quad \text{(SI8)}$$

Then, the Eq. (SI5) can be expressed as a standard form of linear oscillator:

$$\frac{d^2x}{dt^2} + c\frac{dx}{dt} + \omega_0^2 x = A_0 sin(\omega t) \quad \text{(SI9)}$$

where c is the damping constant; ω_0 is the natural frequency; A_0 is the driving acceleration magnitude per mass. It is worth noting that the natural frequency in Eq. (SI7) is a bit different from that found from frequency response function or susceptibility function [*Hilpert et al.*, 2000]. Because this defined frequency is merely to resemble linear oscillator, it will be not the exact natural frequency in the oscillatory system.

The general solution of Eq. (SI9) is composed of two parts: the complementary function $x_c(t)$ and the particular integral $x_p(t)$:

$$x(t) = x_c(t) + x_p(t) \quad \text{(SI10)}$$

The complementary function $x_c(t)$ is found by equating the driving acceleration A_0 to zero in Eq. (SI9) and solving the associated homogeneous ordinary differential equation. The particular integral $x_p(t)$ is directly solved from Eq. (SI9). The complementary function and particular integral correspond to the unsteady-state and steady-state response of the dynamic system in Eq. (SI9) in a similarity to linear oscillator. In what follows, the unsteady-state response and steady-state response are analyzed, respectively.

Unsteady-state response is the solution of equation:

$$\frac{d^2x}{dt^2} + c\frac{dx}{dt} + \omega_0^2 x = 0 \qquad \text{(SI11)}$$

The complementary function to this equation can be written [*Ogata*, 1998]:

$$x_c(t) = \alpha e^{-ct/2} cos(\omega_1 t) + \beta e^{-ct/2} sin(\omega_1 t) \qquad \text{(SI12)}$$

where $\omega_1 = \left(\omega_0^2 - \frac{c^2}{4}\right)^{1/2}$, and α and β are arbitrary constants. The premise for solution (SI12) is $c < 2\omega_0$. It corresponds to an underdamped harmonic oscillation. For the critical damped and overdamped scenarios, the unsteady-state response in Eq. (SI11) does not oscillate at all, and any motion simply decays away exponentially in time. Therefore, it is insignificant on the amplitude of complete solution $x(t)$, and it will not be discussed in this study. For the complementary function in Eq. (SI12), the oscillatory frequency ω_1 is smaller than the undamped resonant frequency ω_0 and this difference is controlled by the damping constant c. The amplitude of the oscillation decays exponentially with time at the rate of $c/2$.

The steady-state response is the particular integral of Eq. (SI9) as time approaches infinity. The form of steady-state solution is [*Ogata*, 1998]:

$$x_p(t) = \frac{A_0}{\left[\left(\omega_0^2 - \omega^2\right)^2 + c^2\omega^2\right]^{1/2}} sin(\omega t - \varphi) \qquad \text{(SI13)}$$

where

$$\varphi = \tan^{-1}\left(\frac{c\omega}{\omega_0^2 - \omega^2}\right) \qquad \text{(SI14)}$$

The particular integral has a constant amplitude independent on t. The sum of particular integral and complementary function is identical to a superposition of two oscillatory modes, one with frequency ω and the other with frequency ω_1.

Combining Eqs. (SI12) and (SI13), the general solution of Eq. (SI9) is:

$$x(t) = \frac{A_0}{\left[\left(\omega_0^2 - \omega^2\right)^2 + c^2\omega^2\right]^{1/2}} sin(\omega t - \varphi) + \alpha e^{-ct/2} cos(\omega_1 t) + \beta e^{-ct/2} sin(\omega_1 t) \qquad \text{(SI15)}$$

The arbitrary constants α and β are determined by the initial conditions in Eqs. (21) and (22), which are:

$$\alpha = -\frac{A_0}{\left[\left(\omega_0^2 - \omega^2\right)^2 + c^2\omega^2\right]^{1/2}} cos\varphi \qquad \text{(SI16)}$$

$$\beta = -\frac{A_0}{\left[\left(\omega_0^2 - \omega^2\right)^2 + c^2\omega^2\right]^{1/2}} \left[\frac{\omega sin\varphi + c \cdot cos\varphi/2}{\omega_1}\right] \qquad \text{(SI17)}$$

The general solution $x(t)$ is the time-dependent mean displacement in the capillary tube in response to excitation. The conversion to dynamic contact angle can be referred to Eqs. (16) and (17). The presentation of dynamic contact angle is more practical and straightforward. Therefore, the dynamic contact angle from approximate analysis and theoretical model will be compared.

Comparison with Previous Studies

Because different acceleration amplitudes are required for unsteady-state response and steady-state response, *Charlaix and Gayvallet* [1992] conducted experiments on investigation of pinned oscillation and sliding oscillation by different magnitudes of excitation as shown in Fig. SI1. A single interface was harmonically driven by periodic pressure force.

In this study, the frequency response $\bar{v}(\omega)/\Delta P(\omega)$ is analyzed with respect to driving frequency at small amplitude oscillations and large amplitude oscillations. Overdamped system and underdamped system are separately considered based on different fluid properties. Only overdamped system is covered in this section for the comparison. The geometric parameters we used are: L_o = 4.5 cm, L_w = 0.5 cm, and R = 0.75 mm. The nonwetting phase used is mineral oil and the wetting phase is fluid solution of 70% glycerol and 30% water. The fluid properties for overdamped system are: μ_o = 1.94×10^{-2} Pa·s, μ_w = 2.47×10^{-2} Pa·s, ρ_o = 970 kg/m^3, ρ_w = 1180 kg/m^3, and σ = 0.039 N/m. The $\Delta P(\omega)$ is composed of capillary pressure and viscous pressure drop in their analysis. The Eq. (20) has to be tuned to fit this condition. The rearranged equation is:

$$\rho_o L_o \frac{d^2x}{dt^2} + 2\rho_o \omega L_o \mathcal{H}_1(x)\frac{dx}{dt} + \rho_w \omega L_w \frac{dx}{dt}\cdot Re\left\{\frac{i\cdot J_0\left(\sqrt{i^3\omega/\omega_c^w}\right)}{J_2\left(\sqrt{i^3\omega/\omega_c^w}\right)}\right\} - \frac{2\sigma}{R}(cos\theta^- - cos\theta^+) = \rho_w L_w A sin(\omega t) + \rho_o L_o A sin(\omega t) \quad \text{(SI18)}$$

The left-hand side is identical to $\Delta P(t)$ they used. For the one interface condition, the left interface can be set as vertical, θ^- = 90°, meaning no capillary pressure in the left meniscus. Therefore, the frequency response in our model is $\bar{v}(\omega)/\Delta P(\omega) = \frac{amp\{dx/dt\}}{amp\{\rho_w L_w A sin(\omega t)+\rho_o L_o A sin(\omega t)\}}$, where $amp\{\cdot\}$ is used to denote amplitude of oscillatory curve. The velocity can be numerically calculated from Eq. (SI18), and the denominator is constant equal to $(\rho_w L_w + \rho_o L_o)A$. It is noted that the equilibrium contact angle was not specified in *Charlaix and Gayvallet*'s work. By reproducing the same result, the equilibrium contact angle we deduced from their work is 46°. The experimental data is well fitted by Eq. (3) in their work with $C(\theta_0)$ as an adjustable parameter. Their fitting equations for single fluid and interface are displayed in Fig. SI1. The peak of red and blue curves is around 18 Hz which is identical for our theoretical model and experimental data. The small difference near the peak is attributed to the consideration of short length of water phase in geometry. L_w is intended to be short to be neglected in their fitting equation. The normalization of the mean displacement is defined as $X_0 = 3x_0/2R$, where x_0 is the amplitude of mean displacement oscillation. In the mean displacement $X_0 < 0.1$, *Charlaix and Gayvallet* [1992] indicated that the model can be treated as linear, but this statement of linear analysis is not necessary convincing to follow. Because the mean displacement in the flow is difficult to control and measure, the use of driving amplitude and frequency as controlling parameters is more convenient. The corresponding relation of acceleration amplitude and driving frequency can be obtained by the analysis of using Eq. (SI18).

Another experiment on the resonance of drop in vertical tube was conducted by *Hilpert and Miller* [1999]. The gravity was considered in the equilibrium contact angle of upper meniscus and lower meniscus. In certain oscillation, the upper meniscus shifted to sliding motion while the lower contact line is in pinned oscillation. The steady-state response was analyzed but the explanation on the sliding motion was not explained. Based on the model in this study, it could be attributed to unsteady-state response of oscillation.

The unsteady-state response of oscillation is rarely considered in previous literature. The validation of this model can be done by a comparison with existing theories in terms of steady-state response. *Hsu et al.* [2012] validated the resonance model by laboratory experiments, and a pressure balance model in quasi-static analysis was established. In their model, the linear approximation of capillary force was implemented in the assumption of small displacement oscillation. In this section, the comparison of our model in Eq. (SI5) with the steady-state frequency response to *Hsu et al.*'s model is implemented. For the

oscillatory motion of drop, the mean displacement follows: $x = x_0 e^{-i\omega t}$. The pressure drop in *Hsu et al.*'s work is identical to the left-hand side terms of Eq. (SI5). Therefore, in consistency with their definition of frequency response function, the function becomes:

$$\frac{x_0}{A}(\omega_c^o)^2 = \left\{\frac{4\sigma sin\theta_0(1+sin\theta_0)^2}{(\rho_o L_o+\rho_w L_w)R^2(\omega_c^o)^2} - \frac{\omega^2}{(\omega_c^o)^2}\left[\frac{\rho_o L_o+2\rho_o L_o\cdot c_1+\rho_w L_w\cdot c_2}{\rho_o L_o+\rho_w L_w}\right]\right\}^{-1} \quad \text{(SI19)}$$

where

$$c_1 = \frac{1}{\sqrt{i^3\omega/\omega_c^o}}\frac{J_1\left(\sqrt{i^3\omega/\omega_c^o}\right)}{J_2\left(\sqrt{i^3\omega/\omega_c^o}\right)} \quad \text{(SI20)}$$

$$c_2 = -\frac{J_0\left(\sqrt{i\omega/\omega_c^w}\right)}{J_2\left(\sqrt{i\omega/\omega_c^w}\right)} \quad \text{(SI21)}$$

The coefficients c_1 and c_2 are now complex value. The dimensionless resonant frequency of the underdamped system in Eq. (SI19) is $\sqrt{\frac{4\sigma sin\theta_0(1+sin\theta_0)^2}{(\rho_o L_o+\rho_w L_w)R^2}}$, which is the same as Eq. (12) in *Hsu et al.* [2012].

Eq. (SI19) is a dimensionless frequency response of the drop in the straight capillary tube. Both wetting and nonwetting phase are prepared immersion liquid. The fluid properties in *Hsu et al.*'s model are: ρ_w = 869 kg/m^3, ρ_o = 2055 kg/m^3, μ_w = 1.3×10^{-2} Pa·s, μ_o = 1.03×10^{-2} Pa·s, σ = 1.48×10^{-2} N/m, θ_0 = 140°. The geometric parameters are: R = 1 mm, L_w = 6.2×10^{-3} m, L_o = 2.38×10^{-2} m. The experimental data and frequency response from both models are presented in Fig. 8. The red curve is wider near the resonant frequency and it means a larger damping than that predicted by *Hsu et al.*'s model [*Hsu et al.*, 2012]; this damping effect of our model is closer to the experimental data. Compared to experimental data, the peak is higher, which could be attributed to a noticeable gravitational effect in experiment.

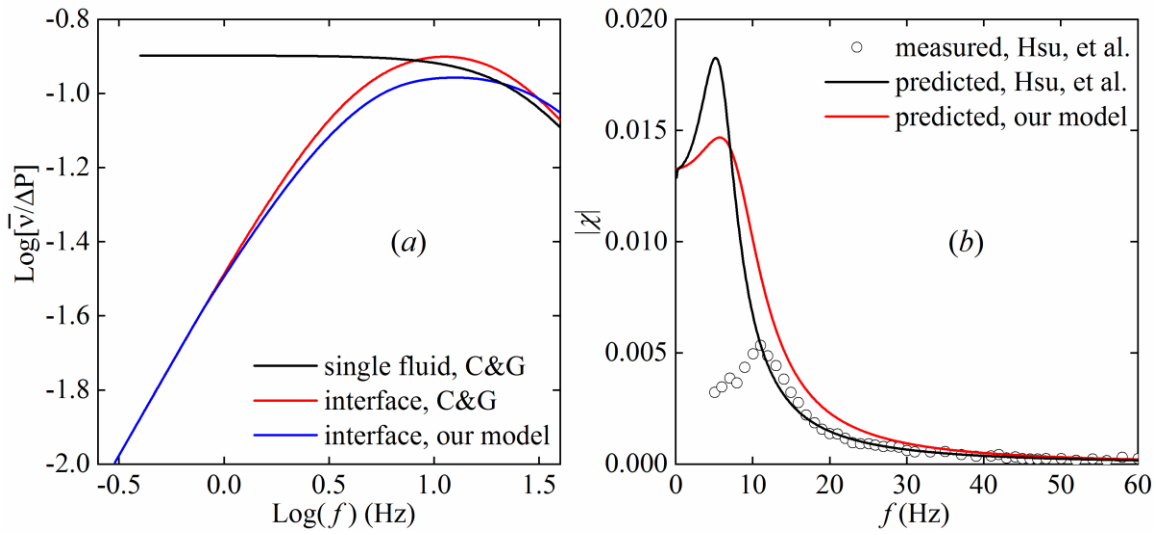

Fig. SI1. (a) The frequency response $\bar{v}(\omega)/\Delta P(\omega)$ obtained at low displacement amplitude in overdamped system. The black curve and red curve come from Eq. (3) in *Charlaix and Gayvallet* [1992] (abbreviated as C&G in legend), fitting well with experimental data. The blue curve is calculated from

our model in Eq. (SI18). (b) Absolute value of the non-dimensional frequency response of a drop in a capillary tube. The measured data and predicted curve are from Hsu et al. [*Hsu et al.*, 2012].

Seismic Acceleration Amplitude

The seismic acceleration for compressional wave and shear wave in liquid systems can be given as [*Pride et al.*, 2008; *Zeng and Deng*, 2020]:

$$A_p \approx 2\omega c_p \frac{\varepsilon_0}{\lambda+1} \text{ and } A_s = \omega c_s \frac{\varepsilon_0}{\lambda+1} \quad \text{(SI22)}$$

where subscripts p and s denote compressional and shear waves, respectively; ε_0 is the initial seismic strain at seismic source, with a type range from 10^{-10} to 10^{-3} for an earthquake; λ is the distance from seismic source; c_p and c_s are compressional and shear wave speed, respectively, which usually can be given as c_p = 3000 m/s and c_s = 1000 m/s; A_p and A_s are the acceleration amplitudes of compressional wave and shear wave, respectively. The frequency band is from 1 Hz to 10^4 Hz. The acceleration induced by internally dynamic events follows [*Pride et al.*, 2008]:

$$A_i = \frac{\mu_o \Delta Q}{4\pi k \rho_0 \lambda^2} \quad \text{(SI23)}$$

where ΔQ is the perturbed volumetric flow rate, k is the hydraulic permeability in porous media. Subscribe i denotes the 'internal' oscillatory source in porous media, compared to the previous 'external' source. ΔQ depends on the pore and throat sizes, and 1/5 fraction of steady-state flow rate is used at here [*Zeng and Deng*, 2020].

Dataset

A spreadsheet titled 'data.xlsx' is contained in this Supporting Information in a separate file. The spreadsheet includes the data of Figures 1-7 and SI1 in paper and Supporting Information. In that file, all data are presented in the same tab and ordered in the same sequence as manuscript. The figure legend and x-y titles are also listed. If there is any question about the data file, feel free to contact the corresponding author Dr. Wen Deng.

References

Charlaix, E., and H. Gayvallet (1992), Dynamics of a harmonically driven fluid interface in a capillary, *Journal de Physique II*, *2*(11), 2025-2038.

Hilpert, M., and C. T. Miller (1999), Experimental investigation on the resonance of a liquid column in a capillary tube, *J. Colloid Interface Sci.*, *219*(1), 62-68.

Hsu, S.-Y., J. Katz, and M. Hilpert (2012), Theoretical and experimental study of resonance of blobs in porous media, *Geophysics*, *77*(5), EN61-EN71.

Ogata, K. (1998), *System dynamics*, Prentice Hall Upper Saddle River, NJ.

Pride, S. R., E. G. Flekkøy, and O. Aursjø (2008), Seismic stimulation for enhanced oil recovery, *Geophysics*, *73*(5), O23-O35.

Zeng, C., and W. Deng (2020), Effect of Subsurface Microseisms on the Motion of Dispersed Droplets in Pores, *J. Geophys. Res.: Sol. Ea.*, *125*(4), e2019JB018783.